Bull Volcanol (1998) 60:38–51 © Springer-Verlag 1998

ORIGINAL PAPER

A. W. Woods · M. I. Bursik · A. V. Kurbatov

The interaction of ash flows with ridges

Received: 20 December 1996 / Accepted: 15 March 1998

Abstract Using both laboratory experiments and theoretical models, we examine the different flow regimes that may develop when an ash flow encounters a ridge. For very small ridges, all the flow may pass over the ridge. For intermediate-size ridges, the flow may be partially blocked, with a fraction of the flow reflected upstream as a travelling bore. In this case, the remainder of the flow, which does pass over the ridge, is hydraulically controlled at the ridge crest. Finally, if the ridge is sufficiently high, then the flow will be totally blocked. New laboratory experiments show that the sedimentation patterns associated with these flow regimes may be very different. Most importantly, flows that involve partial blocking and the formation of upstream propagating bores display enhanced sedimentation upstream of the ridge, analogous to valley-ponded and caldera-fill deposits. In contrast, under some circumstances, if the flow is able to scale a ridge, the deposit may be relatively unaffected by the presence of the ridge. The minimum ridge height that leads to total blocking of the flow increases with mass eruption rate and has a complex variation with distance from the source. In a one-dimensional channel, the minimum ridge height that causes blocking increases with distance downstream. This is because the flow becomes less dense through sedimentation of particles and entrainment of air and so requires less energy to scale a ridge of a particular height. In axisymmetric flow, the minimum ridge height initially decreases with distance downstream as the flow spreads radially, but subsequently increases as the flow becomes less dense through sedimentation and entrainment. A new quantitative model of dilute ash flows propagating over ridges indicates that flows with mass fluxes in excess of 10^8–10^9 kg/s can partially scale barriers as high as 1000 m at distances of tens of kilometres from the source, whereas smaller flows are likely to be totally blocked by such an obstacle. Our results shed new insight on the possible long-range transport mechanism of several large flows including the Ata, Fisher and Aniakchak pyroclastic flows.

Andrew W. Woods (✉)
School of Mathematics, University of Bristol, Bristol, BS8 1TW

Marcus I. Bursik · Andrei V. Kurbatov
Department of Geology, SUNY, Buffalo, New York 14260 USA

Editorial responsibility: M. Rosi

Introduction

The extreme mobility of large ash flows, exhibited in their ability to surmount high topographic obstacles, has presented one of the most confounding problems to physical volcanology. Aramaki and Ui (1966) noted that the Ata pyroclastic flow was able to overtop barriers as high as 800 m at distances of 25 km from the vent. They hypothesized that the flow consisted of a high "fluidized layer" from which material gradually settled over the landscape. Miller and Smith (1977) found that the Fisher outflow sheet was deposited across the Tugamak Range, more than 500 m high at a distance of 15 km from the vent; and the Aniakchak sheet surmounted 700 m high barriers at 20 km. The Mount St. Helens flow although small, overcame transverse ridges as high as 500 m at 10 km from the summit crater (Hoblitt et al. 1981; Fisher 1990; Druitt 1992), whereas the Taupo deposit is found on both sides of ridges over 1000 m high tens of kilometres from Lake Taupo, the vent site (Wilson and Walker 1985).

In drawing an analogy between large ash flows and long-runout landslides, Miller and Smith (1977) envisioned these mobile flows as compact, fluidized bodies, dominated by their momentum attained from a collapsing eruption column and travelling perhaps on a cushion of trapped air. Walker and McBroome (1983) and Wilson and Walker (1985) advocated this same model in studies of the Mount St. Helens blast flow and the Taupo ignimbrite. However, many detailed studies of the Mount St. Helens deposit, including those of Hoblitt et al. (1981), Waitt (1981), Brantley and Waitt

(1988), Fisher (1990) and Druitt (1992), advocate models of the flow as a highly expanded and turbulent gravity-driven flow.

Several recent models have treated massive ash flows as dilute and highly turbulent currents (Valentine 1987; Valentine and Wohletz 1989; Bursik and Woods 1996). Such models may be particularly relevant for massive ash flows produced from collapsing fountains. This is because collapsing fountains tend to be dilute as a result of the decompression and entrainment of air above the vent. Indeed, model calculations predict densities of 10 kg/m^3 in the collapsing fountain (Bursik and Woods 1996), which suggests a particle volume fraction of less than approximately 0.01. Although part of the flow could become dense again, particularly near the lower boundary, the flows are highly turbulent and energetic. Therefore, much of the volume of the flow may remain dilute. This dilute part of the flow will then propagate laterally until it has deposited a sufficient mass of particles to become buoyant and form a coignimbrite cloud. It is the dynamics of this dilute part of the flow that we examine in this paper.

Bursik and Woods (1996) have demonstrated that the dynamics of the dilute flow are largely controlled by the mass eruption rate and the flow density. In turn, the flow density depends upon the mass of air entrained into the fountain and the flow (Smith 1960) and the rate of sedimentation of the ash particles from the flow (Valentine 1987; Valentine et al. 1990; Dade and Huppert 1996; Bursik and Woods 1996). Model calculations (Sparks et al. 1978; Bursik and Woods 1996) indicate that for eruption rates the 10^8–10^{10} kg/s, massive and dilute ash flows may propagate at speeds 10–200 m/s. Since such eruptions typically persist for as long as several hours to a few days, the runout distance and aspect ratio of the associated deposits may be broadly explained in terms of the eruption duration, the mass eruption rate and the particle sedimentation speed.

The present paper represents a continuation of the study by Bursik and Woods (1996) by examining the role of topography in their model of a dilute ash flow.

Field evidence demonstrates that ash flows are able to surmount topographic barriers and deposit thick valley-ponded ignimbrite and thin hilltop veneers (Wilson and Walker 1985). Numerical studies concur that ridges and caldera walls may have a dominant impact upon the propagation of ash flows (Valentine et al. 1992; Giordano and Dobran 1994). The numerical calculations have illustrated that dilute ash flows may be able to surmount some topographic obstacles, whereas with higher barriers, partial blocking of the flow occurs (Valentine 1987). However, there is a wide and largely unexplored range of flow regimes that may develop as ash flows interact with topographic barriers. Furthermore, the impact of these different flow regimes upon ash deposition patterns and the associated evolution of the flow density is not well understood. Analogue experimental studies of finite, particle-laden aqueous currents (Woods and Bursik 1994) have illustrated that topographic obstacles modify runout distances and sedimentation patterns. Such experiments do not include the effects of compressibility, which may occur in real ash flows, but dynamical scaling of the flow and settling speeds, show that they represent good analogues of the transport and sedimentation of dense particles by a ground current, and many effects are common to ash flows (see below). These laboratory experiments have also identified that topographic obstacles may cause the head of the flow to break up into numerous units, with a fraction of the head propating over a topographic obstacle and another fraction being reflected by the obstacle (cf. Lane-Serff et al. 1995).

In this paper we apply the techniques of hydraulics to understand the fundamental controls exerted by topographic barriers upon the maintained ash flows that follow the head, and to identify their impact on ash deposition. Our approach of combining analogue laboratory experiments with supporting theoretical models is complementary to previous numerical simulations and builds upon the hydraulic models suggested by Freundt and Schmincke (1985) and Levine and Kieffer (1991).

Many massive ash flows tend to spread radially from the vent. However, since the controls exerted by ridges on linear and radially spreading flows are very similar, for convenience in our experiments we have examined the motion of one-dimensional channelled flows. We then use the models derived from our experimental results to examine the motion of both radially spreading and one-dimensional channelled ash flows. First we examine the different types of flow that may develop as an analogue laboratory current passes over a ridge. This provides the framework for understanding the more complex dynamics of a sedimenting current in which the density relative to the environment gradually decreases with distance from the source. We then analyse the deposition of suspended particles from a steady current propagating (a) along a near-horizontal slope and (b) over topographic obstacles. Finally, we combine models of ash deposition and of the topographic control of ash flows to explore the effects of ridges upon ash-flow propagation and the associated ash deposition. We focus on the interaction of flows with ridges aligned normal to the flow. However, the interaction of the flow with ridges aligned obliquely to the flow may be very different and more complex. This will form the subject of future study.

The experimental system

We studied the motion of one-dimensional, particle-laden saline currents advancing through a tank of fresh water. The experimental perspex tank had dimensions $300 \times 100 \times 20$ cm. We inserted a false bottom into the tank in order to model different terrain (Fig. 1). During each experiment, the tank was filled with water to pro-

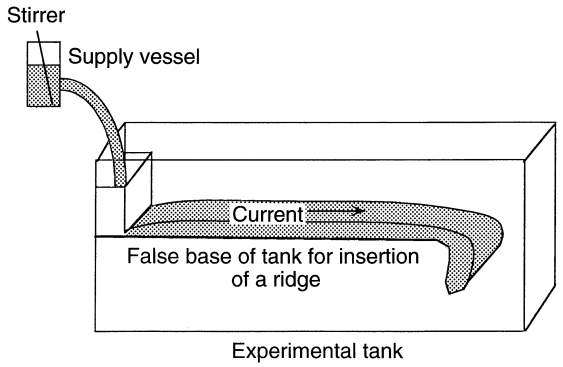

Fig. 1 The laboratory apparatus, including the different topographic controls inserted in the tank

duce a uniform environment, and currents of either aqueous salt solution or particle-laden aqueous salt solution were then discharged into this tank. The fluid was supplied from a 20-l reservoir, entering the tank through a feeder gate (Fig. 1). The particle-laden currents were produced by adding particles of known sizes to the fluid in the feeder reservoir. This was vigorously stirred during discharge to ensure that a uniform well-mixed solution was produced. To focus upon the dynamics, we used saline source fluid of density 1.03 g/cm^3 such that the density of the currents relative to the ambient water did not change significantly as particles sedimented. Effects due to the currents becoming positively buoyant after a certain amount of sedimentation are not considered here, although such effects can be important in pyroclastic flows (Woods and Bursik 1994; Bursik and Woods 1996). The evolution of the flow was recorded by video during each experiment. After each experiment, all of the sediment deposited on the floor of the tank was collected, dried and weighed. The sediment was collected in samples of equal area, spanning the width of the slope (20 cm), each extending 5 cm downslope.

To model particle-laden ash flows, the experiments were designed to have dynamical properties similar to those of ash flows. In particular, the typical Reynolds number of the experiments, uh/ν, was equal to 10^3–10^4 for current depths of order 5–10 cm. Therefore, the flow was highly turbulent, with eddy velocities comparable to mean flow speed. Also, the mean settling speed of the particles of grit used in the experiments was approximately 0.1 cm/s, whereas the average along-current flow speed was 1–10 cm/s. Thus, the current was easily capable of suspending the particles in the flow. This flow regime is directly analogous to that of a dilute massive ash flow. In such flows the typical speed is 10–100 m/s, the flow depth is 100–1000 m, and the flow density is 1–10 kg/m^3 giving Reynolds numbers of 10^7–10^9 and implying a highly turbulent flow. Furthermore, the typical settling speed of ash particles, 0.1–1 mm in size, sedimenting from an ash flow is $\sim$0.1–1 m/s (Bursik and Woods 1996). Therefore, as with our experiments, the turbulence is able to suspend the particles in the flow.

The rate of mixing of the current with the overlying ambient fluid depends on the Richardson number of the current. This represents a balance between the potential energy required to mix and the kinetic energy available for mixing (Ellison and Turner 1959; Turner 1979; Bursik and Woods 1996)

$$R_i = \frac{g\Delta\ h}{u^2}. \tag{1}$$

If the Richardson number of the flow takes very small values (<0.1) then the entrainment becomes significant. However, for larger values of R_i, the entrainment is negligible. In the laboratory experiments, there was a zone of flow establishment of length $\sim$10–20 cm beyond the source, in which the mixing was very vigorous (cf. Wilkinson and Wood 1971). However, downstream of this region, the flow Richardson number increased to values of $\sim$1–10. As a result, the rate of mixing of ambient fluid into the laboratory currents was very small, and the volume flux of the laboratory currents remained nearly constant as they propagated along slope.

Ash flows may propagate as either subcritical or supercritical flows (Bursik and Woods 1996). Subcritical ash flows are relatively deep and slow, with Richardson numbers typically in excess of unity so that any entrainment of the overlying air is negligible. The laboratory experiments therefore provide a good analogy with subcritical ash flows. Many of the phenomena connected with hydraulic control and blocking that we describe in this paper relate to subcritical flows. Therefore, our experiments have direct analogies for the motion of ash flows. In contrast, supercritical ash flows, which propagate at higher speed, have smaller Richardson numbers (0.1–1.0), and therefore they may entrain significantly more air. Although the fractional increase in mass of the current due to entrainment is still small, some caution is required in applying results to supercritical ash flows, because the present experiments can only simulate the initial stages of their propagation, when the effects of entrainment on the density are negligible.

Dynamics of currents flowing over topographic controls

To illustrate the fundamental controls that ridges can have on the motion of ash flows, it is first useful to develop a simple model of our laboratory system (cf. Turner 1979). Later, we extend this model for application to real ash flows, including the effects of sedimentation of particles on the density of the flow relative to the ambient air. In the experiments, a steady dense current propagated along a near-horizontal boundary through a deep layer of fluid of similar but smaller density (Fig. 2). The motion of this current may be described using conservation of mass and momentum.

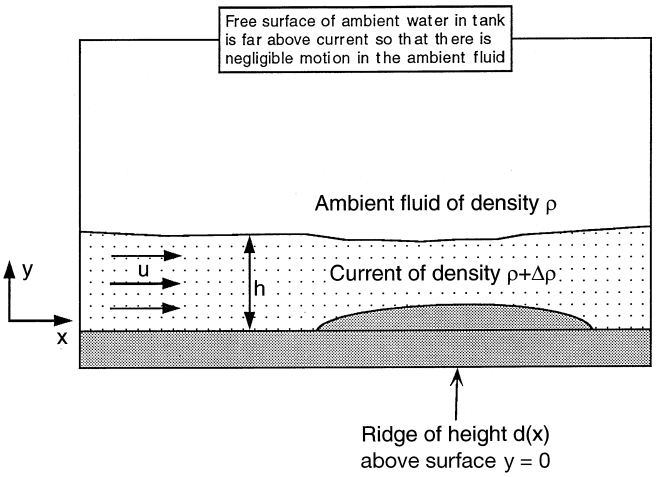

Fig. 2 The model ash flow showing the different flow properties

Equations of motion

Mass conservation

As described above, due to the relatively large Richardson numbers of the experiments, and hence the lack of significant entrainment, to good approximation the volume flux per unit width, Q, is constant,

$$Q = uh \tag{2}$$

Momentum conservation

On a nearly horizontal slope under a deep overlying layer of fluid, the equation of motion for steady flow has the form

$$u\frac{du}{dx} = -\frac{dp}{dx} - (\ \ +\Delta\ \ )g\sin\theta - F, \tag{3}$$

where $p(x, y)$ is the pressure at height y above the slope, and F is the frictional stress on the current. In the laboratory system, the density of the particle-laden saline currents, $+\Delta$, was close to that of the ambient water, ; thus, we can approximate the current density with the value except when calculating terms that are directly dependent on this density difference (the Boussinesq approximation; cf. Turner 1979). The local hydrostatic pressure at height y above the boundary $y = \mathrm{d}$ is given by

$$p(y) = p_a + \ g(H - d - h) + g(\ \ +\Delta\ \ )(h - y), \tag{4}$$

where $d(x)$ is the depth of the boundary above surface $y = 0$, the free surface is at $y = H$ and $h(x)$ is the depth of the current at distance x along-slope. In the experiments, the Reynolds number is of magnitude 10^5–10^6; thus, the currents are turbulent. Therefore, the frictional stress F acting on the current may be expressed in terms of the friction factor $f \sim 0.01 - 0.001$ and the current depth speed, $F \sim fu^2/h$ (Schlichting 1979). For the laboratory currents $F \sim 10^{-2}$ and thus is negligible, in direct analogy with calculations of the motion of ash flows (Bursik and Woods 1996).

If we combine all these simplifications, then the momentum, Eq. (3), may be reduced to the convenient form, using the approximation $dd(x)/dx = \sin\theta$

$$\mathcal{B} = \frac{u^2}{2} + \Delta\ gh + \Delta\ gd, \tag{5}$$

where the Bernoulli integral, $\mathcal{B}$, which represents the energy per unit mass of the flow, is a constant. Combining Eqs. (2) and (5) we deduce that as a steady flow passes over a ridge, the velocity evolves according to the relation (cf. Turner 1979)

$$\mathcal{B} = \frac{u^2}{2} + \frac{\Delta\ gQ}{u} + \Delta\ gd = B_0 + \Delta\ gd, \tag{6}$$

where the quantity

$$B_0 = \frac{u^2}{2} + \frac{\Delta\ gQ}{u} \tag{7}$$

varies with velocity u and takes its minimum value when

$$u = u_c = (\Delta\ gQ/\ \ )^{1/3}. \tag{8}$$

If $u < u_c$, then the flow is called subcritical, whereas if $u > u_c$, the flow is supercritical.

Flow over a ridge

When the flow encounters a ridge, numerous flow regimes may develop depending on the height of the ridge and the flow speed. These different regimes follow from Eq. (6) and were described mathematically by Houghton and Kasahara (1968) in their study of the flow of wind over mountains. Here, we summarise the main results and phenomena in the context of our experiments. However, for completeness, in the Appendix we include a full physical derivation of the different possible flow regimes.

If a subcritical flow encounters a small ridge, then it can surmount the ridge by increasing its speed and lowering the value of the quantity B_0 (Eq. (7)) to compensate for the increase in potential energy, $\Delta\ gd$, such that $\mathcal{B}$ remains constant. If the ridge is sufficiently high that, in order to pass over the ridge, B_0 falls to the minimum value, $B_0(u_c)$, then the flow is described as being critical at the ridge crest; downstream of the crest, the flow may become supercritical (Fig. 3a). This is the highest ridge that the flow can pass over en masse.

If the ridge is higher than the critical height for which the flow is controlled at the ridge crest, then a fraction of the flow is unable to traverse the ridge. Instead, this part of the flow is reflected at the ridge and propagates back upstream as a bore (Fig. 3b). The fraction of the flow that can pass the ridge decreases as the

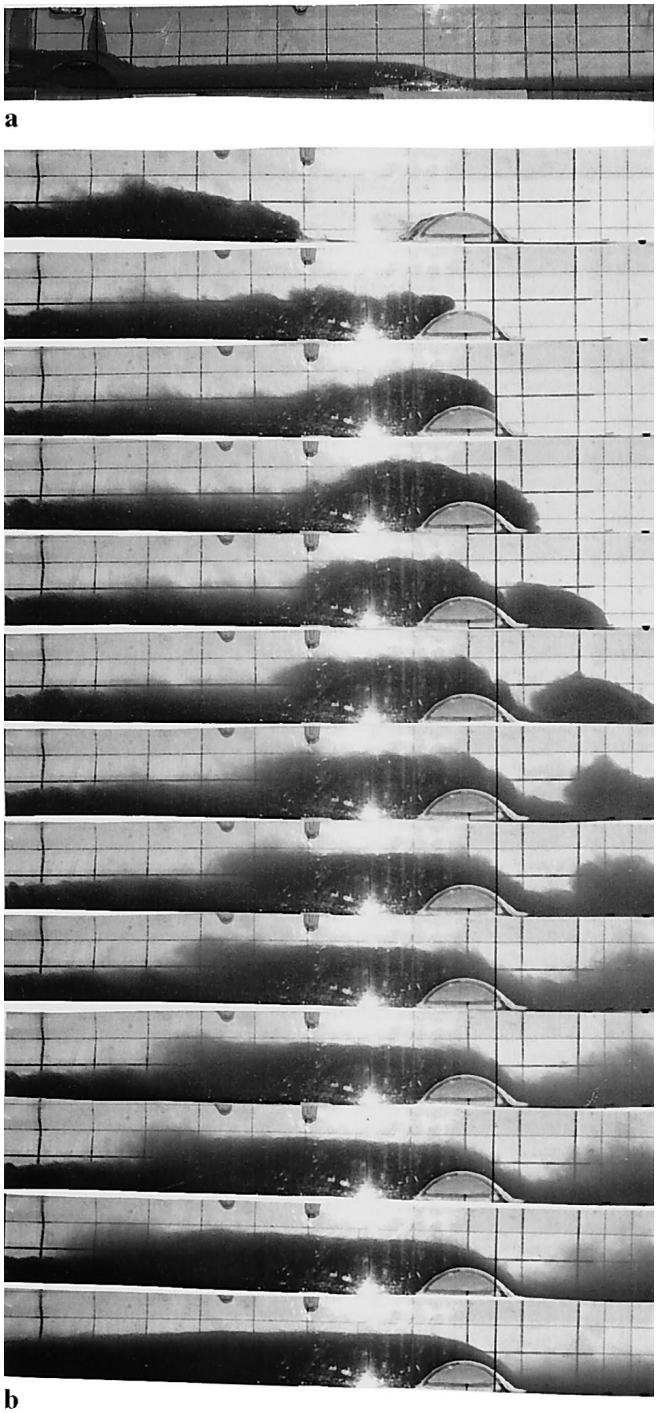

Fig. 3 Photographs of experiments illustrating the **a** transition from subcritical to supercritical flow over a ridge; **b** a sequence illustrating the development of a backward propagating bore, the subsequent deepening of the layer upstream of the ridge and the ultimate flow of the whole current over the ridge. Downstream of the ridge, the flow is supercritical and becomes progressively stronger with time. Note that in a real ash flow the upstream propagating bore may be less dense than the underlying current as a result of sedimentation, and may in fact become buoyant and lift off, thereby preventing sufficient deepening upstream that all the current may pass over the ridge

ridge height increases, until eventually all of the flow is blocked by the ridge. For ridges that are higher than the critical value to block the whole flow, all the flow is reflected at the ridge and no material propagates beyond the ridge crest. Using the hydraulic theory, described in detail in the Appendix, it is possible to calculate the height of a ridge at which the flow first becomes partially blocked and the height at which the flow first becomes fully blocked. We use these results in Application to ash flows passing over ridges, where we apply the model to real ash flows.

More complex terrain

The foregoing discussion has identified the important controls a single ridge may have on an ash flow. However, in general, ash flows propagate over more complex terrain, possibly including several ridges of different heights. In Fig. 4a we present a sequence of photographs to illustrate how a laboratory current gradually adjusts if it encounters two ridges, a relatively small upstream ridge and a larger downstream ridge. The head of the flow, which propagates as a gravity current, splashes up over the ridge, and a fraction continues downstream (cf. Lane-Serff et al. 1995). However, the motion of the steady current following the head becomes somewhat detached from the head as it passes over the ridge; the flow dynamics become controlled by the ridge rather than the head of the flow.

In the experiments, the current is partially reflected by the upstream ridge, and the flow therefore deepens upstream. This deepening continues until all the flow is able to pass over the small ridge. Meanwhile, a large fraction of the flow downstream is reflected by the second ridge. This generates a second large bore which propagates back upstream, causing the flow to deepen in the region between the ridges. This second bore is so deep that it continues to propagate back over the first ridge toward the source. Eventually, the flow upstream of the large ridge deepens sufficiently so that all the flow may pass over this large ridge. The smaller ridge upstream then has a much weaker influence on the steady flow. In the contrasting situation in which there is a large ridge upstream, and a smaller ridge downstream (Fig. 4b), each ridge controls the flow upstream. Indeed, in Fig. 4b the subcritical flow that passes over the second ridge has propagated all the way back to the first ridge. This produces a hydraulic jump in the flow as it changes from the supercritical plunging flow just downstream of the first ridge to the subcritical flow upstream from the second ridge.

Later, we discuss the relevance of these experiments to the propagation of ash flows. One additional effect in ash flows that complicates the discussion is that the reflected bore becomes progressively less dense as it propagates back upstream and deposits particles. As a result, mixing with the underlying, advancing current may be suppressed, and the flow may eventually be-

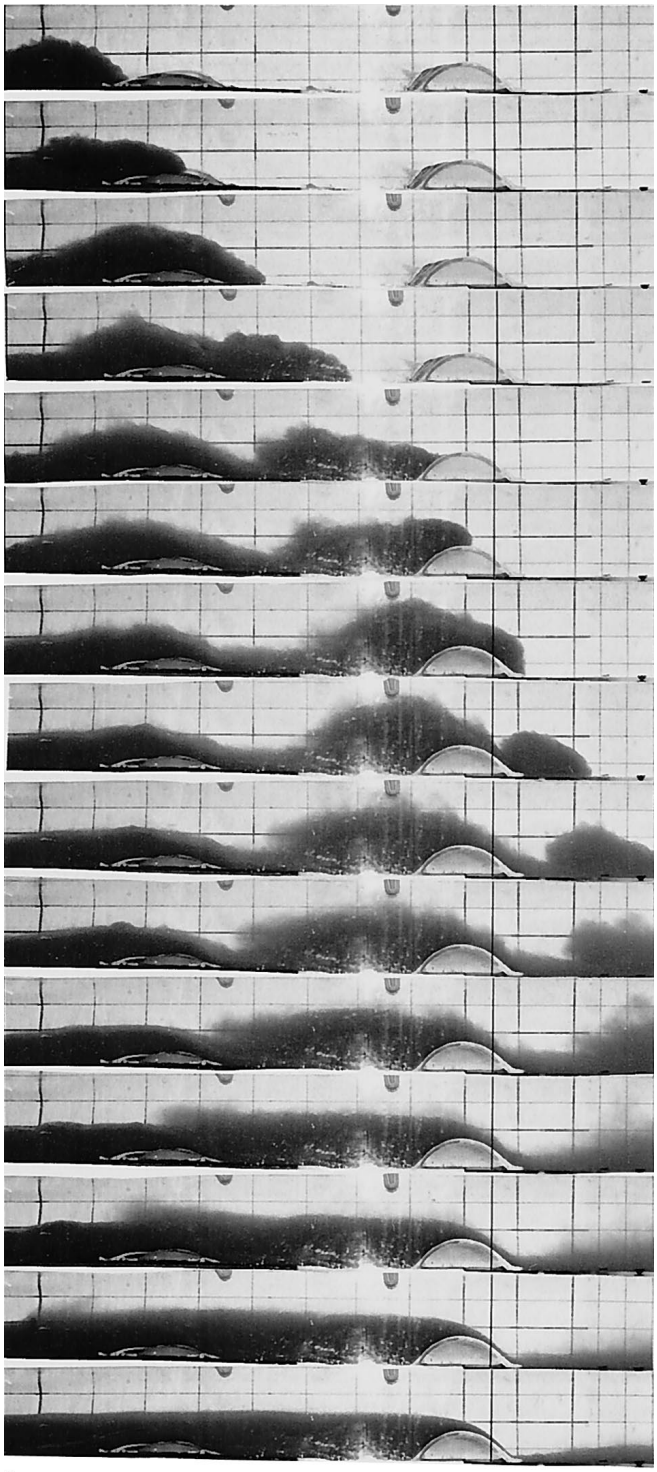

a

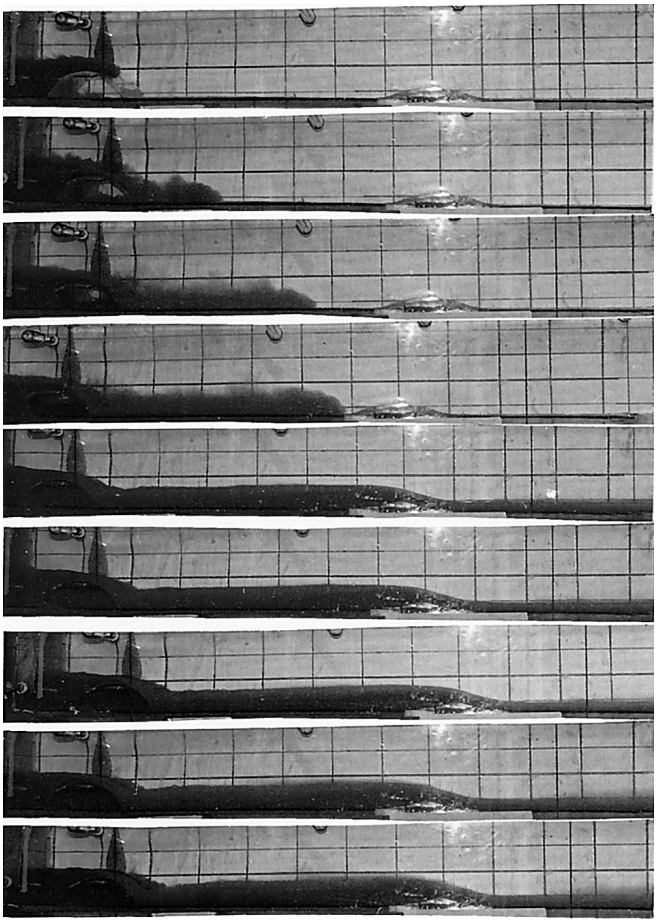

b

Fig. 4a, b The more complex bores and controls on ash-flow propagation that occur when there is more than one ridge present. **a** Sequence shows that, with the larger ridge downstream, the flows are eventually controlled by this ridge everywhere. However, there is a second transient bore that develops upstream of the smaller ridge before the flow is dominated by the downstream ridge. **b** With the larger ridge upstream, each segment of the flow is controlled by nearest upstream ridge

come buoyant. This may reduce the effectiveness of the deepening of the flow upstream of the ridge, thereby limiting the fraction of the flow which can in practice overtop the ridge.

Sedimentation from a steady current on a planar surface

In order to understand how the different topographic controls described previously affect ash deposition, we first examine sedimentation on a uniform surface. This provides a reference with which we can compare the more complex sedimentation patterns as flows move over topography. The present experiments also enable us to test the model of ash flow sedimentation that we applied to predict the properties of some of the largest known ash flows (Bursik and Woods 1996).

Observations

Bursik and Woods (1996) argued that many of the largest ignimbrite deposits in the geological record were emplaced over times 10^4–10^5 s (neglecting pauses

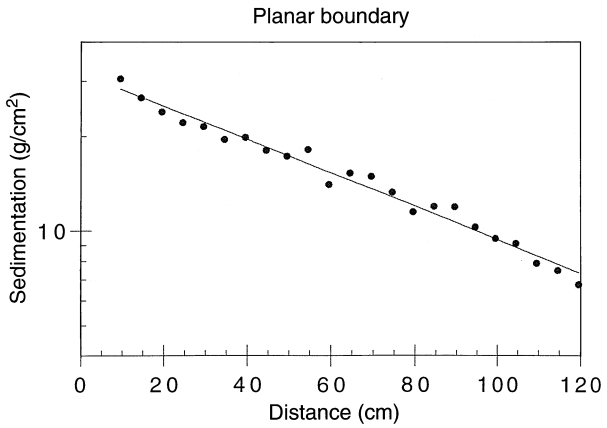

Fig. 5 Variation with along slope position of the mass of sediment on the base of the laboratory vessel, collected during a typical experiments. The experimental data are compared with the exponential decay curve predicted by the theory (see Eq. 11)

between depositional episodes); thus, the majority of the ash deposition occurred from a steady flow. We conducted numerous experiments to examine the deposition from such steady flows and test the basic aspects of their model. In Fig. 5 we show the mass of sediment as a function of the position along the slope, measured in a typical laboratory experiments. To very good approximation, the mass of sediment decays exponentially with distance along the slope. We now show that this is in accord with theoretical predictions.

Theoretical model

As the current propagates along the slope, the mass of particles per unit mass of current decreases by sedimentation. If the mean settling speed of the particles is much smaller than the speed of the flow, then the particles will mix well in turbulent suspension. In our experiments, we used sieved silicon carbide grinding particles with a mean grain size of ~ 100 μm and a mean settling speed of ~ 0.1 cm/s. In contrast, the mean speed of the flow was typically 5 cm/s, so that in our experiments, as with large ash flows (Valentine 1987; Sparks et al. 1978), the particles were well mixed throughout the flow. Hazen's law of sedimentation (1904) suggests that for such a flow, the mass flux of particles, M, decreases at the rate

$$\frac{dM}{dx} = -\frac{v_s M}{Q}, \tag{9}$$

where v_s is the characteristic settling speed of the particles and Q is the volume flux per unit width. Equation (9) suggests that if, as in our experiments, the volume flux of the current remains nearly constant, then the mass flux of particles in the current should decay according to the relation

$$M = M_0\left(1 - \exp\left(\frac{-v_s x}{Q}\right)\right) \tag{10}$$

and the rate of deposition of sediment, S, per unit distance along slope should decay with distance according to

$$S(x) = \frac{M_0 v_s}{Q}\exp\left(\frac{-v_s x}{Q}\right), \tag{11}$$

where M_0 is the initial mass flux of particles. In Fig. 5 we successfully compare the predicted sediment mass (Eq. (11)) with the experimentally measured sediment deposit. We deduce that, for flows in which there is negligible entrainment, the rate of sedimentation depends simply upon the sedimentation speed and the volume flux. The experimental result corroborates the ash flow model used by Bursik and Woods (1996) to estimate (to leading order) deposition patterns and maximum runout lengths in several of the largest historical ignimbrite eruptions. In that study the effects of a grain-size distribution on the sedimentation and dynamic evolution of the flow is also discussed. The key result is that the flow and deposit gradually become more fine grained with distance from the source, although at any point in the flow there is a wide range of grain sizes in the deposit due to the turbulent suspension of the particles. We now examine how the sediment deposition changes if topographic obstacles are present.

Sedimentation over topographic obstacles

Small ridges

In a channel of fixed width, the rate of sedimentation from a steady, non-entraining particle-laden current decays exponentially from the source at a rate that depends only on the volume flux and sedimentation speed. If the flow is able to pass over a ridge *en masse,* then the volume flux upstream and downstream will be the same; thus, the sediment deposit should decay exponentially from the source as in the absence of the ridge (Eq. (11)). We have tested this prediction with an experiment in which a subcritical flow passed over a small ridge, was just controlled at the ridge crest, and became supercritical downstream (see Fig. 3a). Figure 6a illustrates that, to very good approximation, the sediment mass does indeed decay nearly exponentially with alongslope distance; there is no significant signal of the presence of the ridge. Although this result is significant, the Richardson numbers of the experimental currents remain small; thus, there is negligible entrainment into the flow. In contrast, in a real ash flow, the supercritical flow downstream may begin to entrain air, because the Richardson number decreases (Woods and Bursik 1994). Therefore, the rate of sedimentation may begin to decrease somewhat more rapidly with distance downstream (see below).

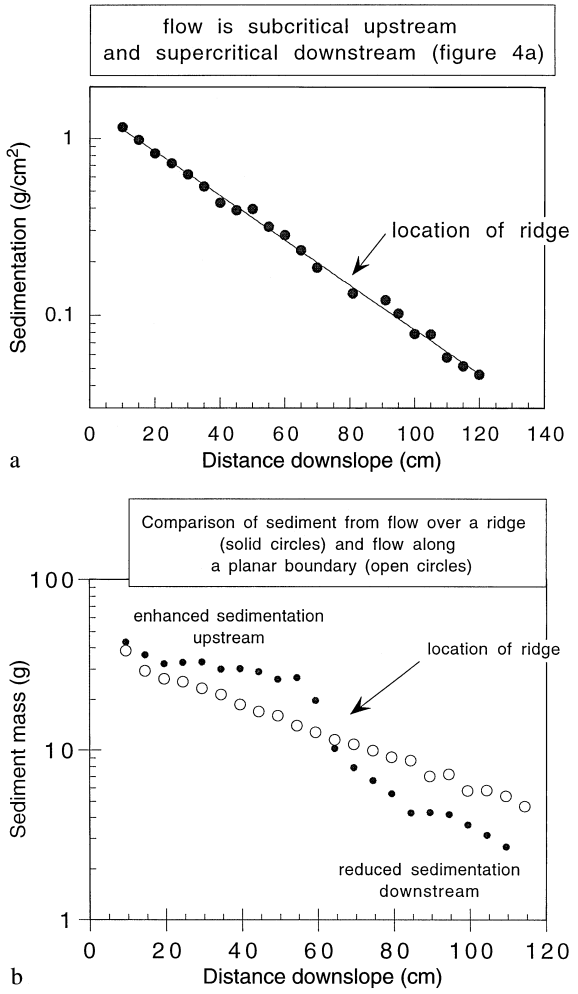

Fig. 6a, b The variation of the sediment deposit as a function of the distance alongslope in a current passing over a ridge. **a** The flow is subcritical upstream and supercritical downstream of the ridge (see Fig. 4a). The deposit shows very little signal of the ridge presence in accord with the theory. **b** The flow was partially reflected at the ridge and therefore the sediment upstream of the constriction is enhanced. For comparison, the results from an experiment on a flat slope are also shown

Partially blocked flow

If the flow has insufficient energy to pass over a ridge *en masse,* then a bore propagates upstream, and the volume flux supplied downstream of the ridge is smaller than that upstream of the bore (Fig. 3b). As a result, much more of the particulate load remains upstream of the ridge, producing a very asymmetric deposit. Also, since the volume flux is smaller downstream of the ridge, the mass of deposit decays more rapidly with distance than it does upstream (Eq. (11); Fig. 6b).

The amount by which the distribution of a deposit is affected by partial blocking depends on the duration of the flow in comparison with the time required for the upstream propagating bore to reach the source or possibly to become buoyant and lift off (see Flow over a ridge). If the flow is able to deepen sufficiently upstream so that all the flow can eventually overtop the ridge, then the deposit will be dominated by the steady state in which the subcritical flow upstream feeds the supercritical flow downstream. If the flow subsequently becomes subcritical further downstream, then, noting possible effects of entrainment (see below), the deposit may not be greatly affected by the ridge (Fig. 6a). However, if the eruption time is relatively short, or the flow is never able to fully overtop the ridge, then a much more asymmetric deposit will result (Fig. 6b).

Sedimentation across changes in slope angle

In addition to flows over smooth ridges, we examined the effect of a decrease in slope, such as occurs in flows propagating down the flanks of a volcano onto a plain. However, for small changes in slope (a few degrees) the steady flow does not entrain large quantities of fluid at the slope break; thus, the volume flux of the current remains nearly constant across the slope break. As a result, we found that, to good approximation, the mass of sediment continues to decay exponentially with distance as in the case of a planar slope.

Application to ash flows passing over ridges

The model presented herein enables us to study the motion of an ash flow passing over a ridge. We can apply the theory (see Dynamics of currents flowing over topographic controls and the Appendix) to calculate the minimum ridge height that can totally block a flow. Our model of steady flow over a ridge enables us to calculate this height. This minimum ridge height will block the flow only if the flow is just critical (see Flow over a ridge). A supercritical flow has greater total energy, and the ridge only partially blocks the flow, so that a fraction can propagate over the ridge. To apply this result, we first adapt the theory presented in Dynamics of currents flowing over topographic controls and the Appendix for application to the motion of ash flows. We analyse both one-dimensional and axisymmetric flows, using the equations describing the steady motion of an ash flow (Bursik and Woods 1996).

One-dimensional ash flow

Bursik and Woods (1996) showed that if a flow propagates subcritically, then entrainment is negligible. Therefore, in a one-dimensional channel, the volume flux per unit width, Q, remains constant at its initial value

$$Q = Q_0. \tag{12}$$

Also, by analogy with Eq. (3), the momentum equation has the form (cf. Turner 1979)

$$hu\beta\frac{du}{dx}=gh(\alpha-\beta)\frac{d(h+d)}{dx}-\frac{1}{2}gh^2\frac{d\beta}{dx}-f\beta u^2, \quad (13)$$

where β is the current density, α the ambient density, d is the height of a ridge and $f\beta u^2$ is the frictional force acting on the current. The second term on the right-hand side represents the acceleration produced by the decrease in buoyancy of the flow with sedimentation (Bursik and Woods 1996). Unless the terrain is particularly rough, the frictional force is small and to leading order may be neglected. On rough terrain, the flow dynamics may be more complex, with local flow separation events developing and possibly changing the efficiency of sedimentation; such effects will form the subject of future study.

As previously shown, we can define a volumetric Bernoulli energy density

$$\mathcal{B}_v=\frac{u^2}{2}+\frac{g'Q}{u}+g'd, \quad (14)$$

where the reduced gravity is now given by $g'=g\frac{\beta-\alpha}{\beta}$. Using Eqs. (12) and (13) it follows that, in an ash flow, the Bernoulli energy density evolves with distance according to the relation

$$\frac{d\mathcal{B}_v}{dx}=\frac{dg'}{dx}\left[\frac{(2\alpha-\beta)Q}{2u\alpha}+d\right]. \quad (15)$$

This equation identifies how the sedimentation of ash, which reduces the relative density of the flow, g', leads to a decrease in the Bernoulli energy density. Since the flow density evolves significantly only over the whole runout distance of the flow, then the Bernoulli energy density also changes significantly only over distances comparable to the length scale of the whole flow. Therefore, in large ash flows, which travel tens of kilometres from the vent, the change in Bernoulli energy density as the flow passes over a typical ridge, 2–5 km long, is relatively small. Thus, to good approximation, we may use the local value of the Bernoulli function (Eq. (14)) to analyse the flow over a ridge.

The rate of sedimentation of ash from the flow may be described using the model presented in sedimentation from a steady current on a planar surface, but including the effects of the multiple-grain-size distribution. Bursik and Woods (1996) have shown that this leads to an expression for the density of a subcritical ash flow as a function of the distance x from the source

$$\beta=\frac{P}{RT}\left[1+\frac{1-n_0}{n_0}\exp\left(-\frac{1}{Q}\int_0^x\bar{v}_s\,dx\right)\right], \quad (16)$$

where P is the atmospheric pressure, T the flow temperature, R is the gas constant of the flow, n_0 is the initial gas mass fraction of the flow and $\bar{v}_s$ is the mean settling speed of the ash, which is a function of distance from the source. Using Eqs. (15) and (16) we can calculate the value of g' and $\mathcal{B}_v$ at each point in the flow. The analysis presented in Dynamics of currents flowing over topographic controls and the Appendix (cf. Fig. A2) may then be applied locally to examine the interaction of the ash flow with ridges of different heights. In particular, for a flow with volume flux Q per unit channel width, the minimum ridge height required to totally block the flow has the value

$$d(x)\sim 2.1\left(\frac{Q}{g'(x)}\right)^{1/3}. \quad (17)$$

This height increases with distance downstream as a result of the sedimentation of clasts and the associated reduction in the density of the flow, which enables the flow to scale progressively higher obstacles (Fig. 7a). The grain-size distribution in the flow has an important influence on the rate of sedimentation and hence the rate at which the density of the flow decreases. Firstly, although the flow becomes progressively finer grained

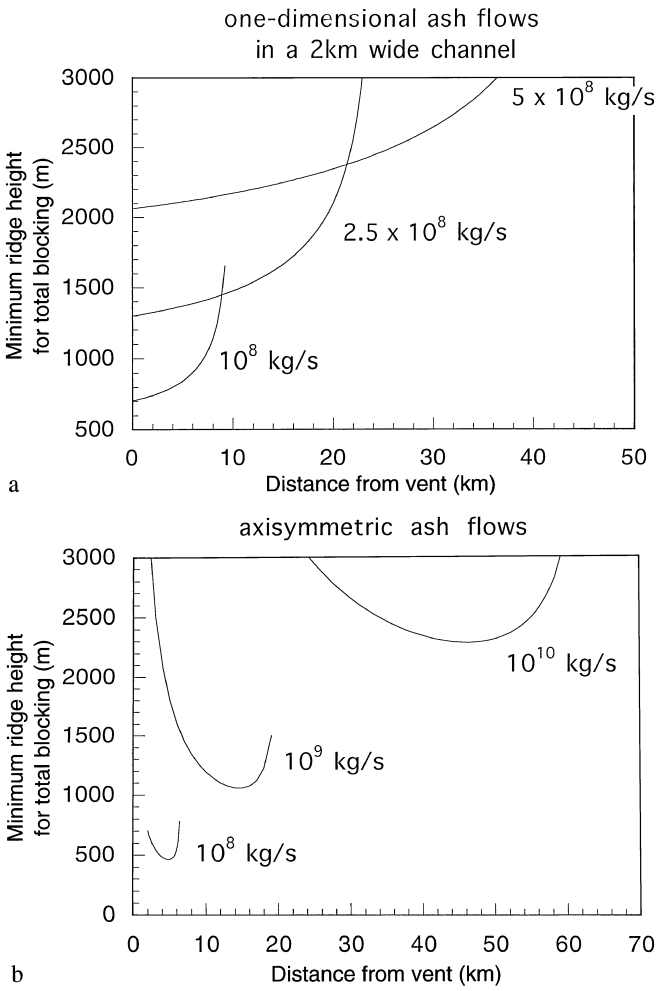

Fig. 7 Calculation of the minimum height of a ridge that will totally block a subcritical ash flow in **a** a one-dimensional channel, and **b** a radially spreading current. Mass fluxes are indicated on the curves

as it propagates from the source, if it is partially blocked by a ridge, then the reflected part of the flow will lead to enhanced sedimentation of the fine-grained material near source. Secondly, in a more fine-grained flow, the sedimentation is slower; thus, a flow of given mass flux is required to propagate much farther before the density has fallen sufficiently to scale a ridge of given height. Thus, the presence of topographic obstacles close to the source may actually lead to blocking and enhanced sedimentation of a fine-grained flow near source, whereas a coarser flow may be able to pass over the ridge.

Also note that if the flow becomes supercritical at some point, then the ensuing entrainment of air causes the density of the flow to decrease toward that of the ambient density more rapidly, and the volume flux in the flow increases. Both of these effects lead to an increase in d (Eq. (17)). We deduce that as supercritical flows evolve, they are able to surmount progressively higher ridges than are their subcritical counterparts.

The results presented herein provide a leading-order guide to the blocking of the flow. However, once the blocking has started, and the bore propagates back upstream, the density of the flow that arrives at the ridge may evolve. Indeed, the flow may become density stratified because of the smaller mass of ash in the bore propagating upstream over the oncoming flow. More detailed study is beyond the scope of the present work, although we note that such stratification of the flow, with a particle-laden underflow and a less dense bore, was observed in the experiments (e.g. Fig. 4).

Radially spreading currents

In the absence of channelling, many ash flows spread approximately radially from the vent. We now extend our model to investigate the effects of ridges on such axisymmetric flows. The Bernoulli energy density for a radially spreading flow has the form

$$\mathcal{B}_{vr} = \frac{u^2}{2} + \frac{g' Q_r}{ru} + g' d, \tag{18}$$

where Q_r represents the total volume flux per radian, $Q_r = uhr$. Using the steady momentum equation for a radial flow (e.g. Bursik and Woods 1996; Bonnecaze et al. 1995), it follows that a subcritical flow evolves with radius r according to the law

$$\frac{d}{dr}\left[\frac{u^2}{2} + \frac{g' Q_r}{ru} + g' d\right] = \left[\frac{(2\alpha - \beta) Q_r}{2u\alpha r} + d\right]\frac{dg'}{dr}, \tag{19}$$

where again we neglect the effects of friction and entrainment. Using a similar method as for the one-dimensional flows, the minimum ridge height that can totally block a flow is given by

$$d_{mr}(r) = 2.1\left(\frac{Q^2}{g' r^3}\right)^{1/3}. \tag{20}$$

The density of subcritical flows evolves mainly as a result of sedimentation. Applying the same model as in one-dimensional ash flows, but adapted for a radially spreading flow (e.g. Bursik and Woods 1996), we can therefore calculate the minimum ridge height for total blocking (Eq. (20)). We find that initially this ridge height decreases as a result of the increase in radius of the flow (Eq. (20); Fig. 7b). However, farther from the source, after the flow has deposited a substantial fraction of its particles, its density approaches that of the ambient air. Thus, the flow is able to surmount increasingly high ridges without being fully blocked. Indeed, for mass eruption rates of 10^8–10^9 kg/s, we predict that the flow is able to overtop obstacles well over 1000 m high. Again, the location of such obstacles ahead of the source will determine the fraction of the flow that is partially blocked by the ridge, and in turn this depends on the grain-size distribution of the flow (see above).

Implications for deposits

The above results suggest that, in many cases, large ash flows are only partially blocked by high ridges, over 1000 m in elevation, and that a fraction of the flow is able to pass over such ridges, especially if located far from the vent. This result is consistent with the field observations described in the Introduction. The formulae presented in this section illustrate that the minimum ridge height for blocking increases with the mass flux of the flow. For eruption rates in excess of 10^8–10^9 kg/s, our calculations (Fig. 7) show that typically a fraction of all ash flows will be able to propagate over ridges even 1000 m high. Only in eruptions with lower mass flux, and flow conditions near the critical speed $U = 1$ (see Appendix), is the flow likely to be totally blocked by a ridge. Given that in most cases part of an ash flow may scale even very high ridges, we now consider how the ridge might impact the sediment deposit.

In Sedimentation over topographic obstacles, we showed that partial blocking of a flow may lead to a much thicker deposit upstream of a high ridge. Such partial blocking may explain the origin of valley-pond and crater-fill deposits, which are often observed (Wilson and Walker 1985). Also, the reflected part of the flow may carry fine-grained material back upstream, leading to anomalous deposition of fine material near the source, in contrast to an unobstructed flow that becomes progressively more fine grained with distance from the source. In our experiments, we also found that, if all the flow overtopped the ridge, then the flow deposit has similar properties upstream and downstream of the ridge (Fig. 6). In a real ash flow the process may be somewhat more complex. In particular, if flow is controlled at the ridge crest, then downstream of the ridge the flow may become supercritical. Depending on the conditions farther downstream, this flow may continue as a supercritical flow or may adjust to become subcritical (Figs. 4, 8). If the flow adjusts to be-

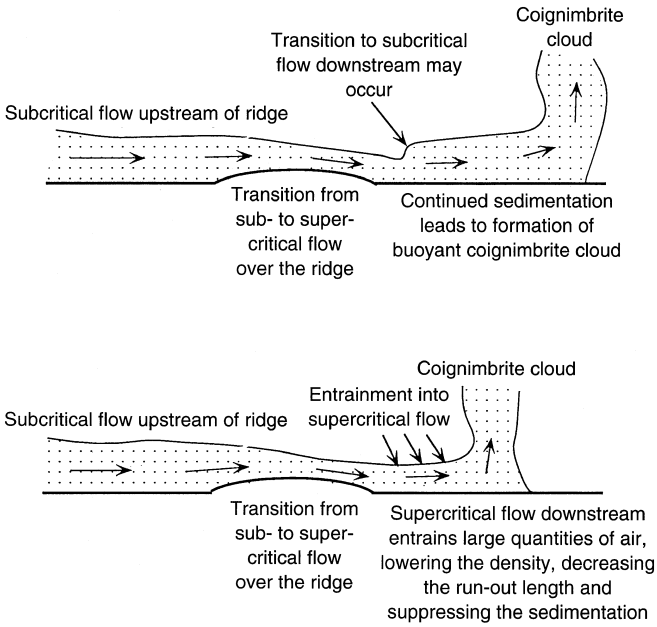

Fig. 8 Diagram shows how the flow and deposit may vary as a function of the presence of a ridge. Depending on the terrain downstream from the ridge, the flow may propagate as a subcritical or supercritical flow after passing over the ridge, and these two flow regimes will lead to different runout lengths and deposition patterns (cf. Woods and Bursik 1994)

come subcritical, then, as in the experiments in sedimentation over topographic obstacles, the deposit will be largely independent of the ridge. However, if the flow remains supercritical, then it will evolve toward very low Richardson numbers and may entrain large quantities of air (Fig. 8). As a result, the particles will become more dilute, and the flow will deposit material more slowly than the corresponding subcritical flow (see aforementioned section). Also, the flow density decreases toward that of the air much more rapidly, reducing the runout length of the flow (cf. Bursik and Woods 1996). Even though the flow might surmount the crest (cf. Fig. A4), the flow deposit may not extend as far beyond ridges as in other directions where there are no topographic controls and the flow can remain subcritical (Fig. 8).

Conclusion

We carried out a series of experiments to examine the control of topography upon the propagation of ash flows. We have shown that ash flows may readily surmount small ridges, and that there may be little indication of the ridge recorded in the thickness variations of the deposit. For larger ridges, only a fraction of the flow can surmount the ridge, and the remainder of the flow is reflected back from the ridge toward the source in the form of a bore (Fig. 9). In this case the ash deposit may be asymmetrically distributed about the ridge, with an unusually thick deposit upstream of the ridge and a rapidly thinning deposit downstream. Calculations suggest that large ash flows, with eruption rates in excess of 10^8 kg/s, can be totally blocked by ridges only higher than approximately 1000–1500 m. Since many ridges are not this high, we expect that, in general, ash flows will partially overtop ridges, as is observed in many deposits (see Introduction). This result is particularly true far downstream of the source, since the flow becomes progressively less dense through sedimentation and thus is able to surmount progressively higher ridges. Indeed, eventually the flow becomes less dense than the surrounding atmosphere and will lift off to form a fines-enriched coignimbrite cloud. Therefore, as they approach their distance of maximum runout, ash flows can surmount high ridges, consistent with observations that the Ata, Fisher, Aniakchak and other large flows were able to overtop extremely high obstacles at great distances from the vent (see Introduction).

Our analysis has identified some of the fundamental effects of ridges upon ash flows. Although the different phenomena are somewhat simplified, they provide a framework for further detailed study of ash-flow interaction with topography. There are many other complex effects that may be induced by ridges, particularly those caused by their lack of regularity and continuity. These effects include flow diversion, as often occurs in smaller

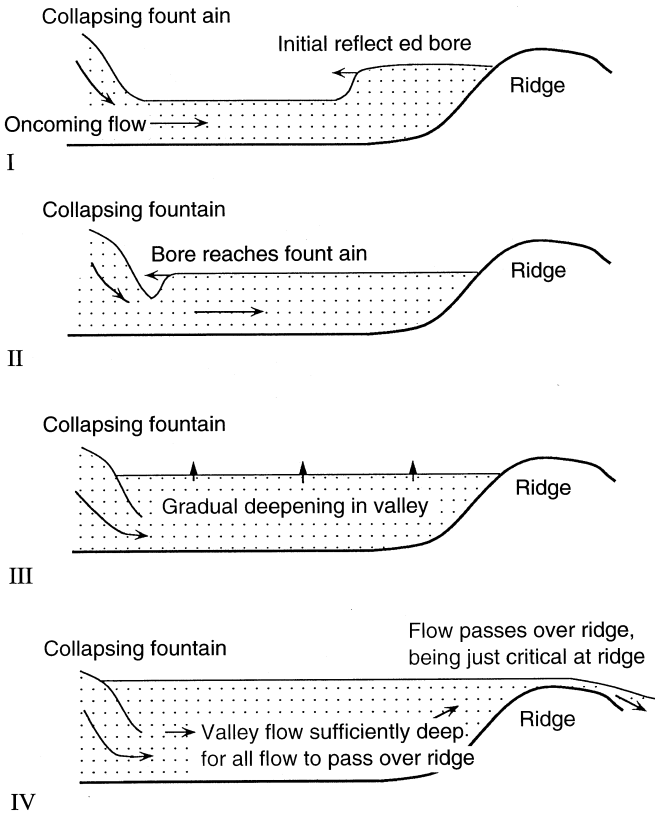

Fig. 9 Illustration of the adjustment of the flow as it passes over a ridge, deepens upstream and eventually passes over the ridge

flows (e.g. Druitt 1992) or when the flow encounters a ridge at an oblique angle (e.g. Kneller et al. 1991). Another important issue concerns the evolution of the leading head of an ash flow, which is different from the main steady flow. Our experiments, and those of Lane-Serff et al. (1995) and Woods and Bursik (1994), suggest that a fraction of this head is able to surmount high obstacles, and that the head becomes detached from the main flow as it passes over such a ridge. These problems will be the subject of future study.

Acknowledgements This research was supported by grant EAR-9316656 from the National Science Foundation. We thank reviewers for their insightful comments.

Appendix: Hydraulics of flows over ridges

In this Appendix, we use the Bernoulli integral $\mathcal{B}$ to analyse the flow over a ridge and thereby establish conditions under which the flow is partially and fully blocked by the ridge. In Fig. A1, we have plotted the variation of B_0 (Eq. (7)) with the velocity u for a given volume flux Q. The energy B_0 has a minimum value when the velocity

$$u = u_c = (g'Q)^{1/3}, \tag{A1}$$

where the reduced gravity g' is defined as $g' = \frac{\Delta\ g}{}$.

This critical speed u_c coincides with the speed of interfacial gravity waves propagating on the surface of the current. For each value of $B_0 > B_c$ there are two possible values of the current speed. If the current speed $u < u_c$, then the flow is slow and deep (subcritical flow). If the speed $u > u_c$, then the current is fast and shallow (supercritical flow).

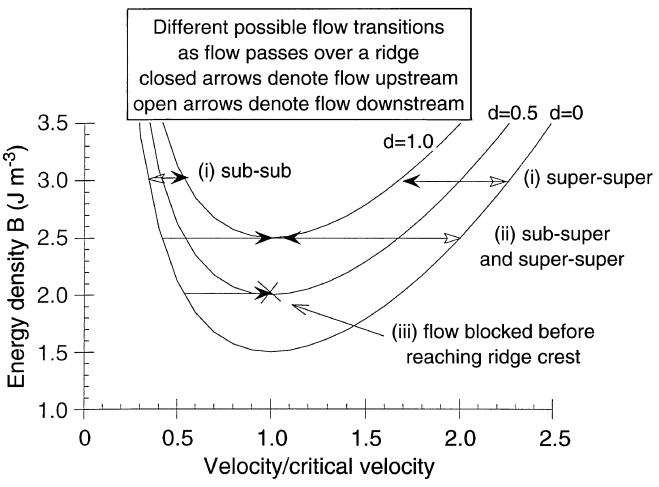

Fig. A1 Variation of the Bernoulli energy integral as a function of the velocity of a current ot fixed volume flux, illustrating the subcritical and supercritical flows. Curves are shown for three fixed values of the elevation of the floor, illustrating how the current velocity evolves with floor elevation. In (*i*) as the depth of the ridge increases, the flow evolves toward the critical flow but remains either sub- or supercritical. In (*ii*) the flow becomes just critical at the point of maximum elevation of the ridge, and then may undergo a transition to the supercritical flow branch. In (*iii*) the flow becomes critical before reaching the top of the ridge and therefore is unable to pass over the ridge as a coherent current

For a given flux Q, both the subritical and supercritical flows have greater energy per unit mass than the corresponding critical flow. This additional energy may be converted to potential energy to lift the flow over a ridge. Therefore, as the flow propagates over the ridge, the current evolves toward the critical flow. This is indicated in Fig. A1, in which the Bernoulli energy density is shown for flow at three different elevations on the ridge. The lines with solid arrowheads illustrate how the flow velocity evolves as the flow moves up the ridge. The arrows with open heads indicate the subsequent evolution of the flow as it descends from the ridge. Numerous flow regimes may develop depending on the elevation of the ridge and the criticality of the flow upstream of the ridge.

Small ridges – smooth flow

If the flow is sufficiently energetic or the ridge is sufficiently small, then all the flow is able to pass over the top of the ridge. As the flow advances ahead of the ridge, it adjusts smoothly back to the flow regime upstream of the ridge (Fig. A1, case (i)).

If the energy is smaller or the ridge is higher, then the flow may become just critical at the ridge crest (line (ii), Fig. A1). This ridge height is the maximum that the flow is able to surmount *en masse* and is given by the condition that the flow just becomes critical at the top of the ridge, so that

$$d = \left(\frac{1}{\Delta\ g}\right)\left(B - \frac{3}{2}\ \ (g'Q)^{2/3}\right). \tag{A2}$$

The analysis may be simplified by scaling the upstream velocity by the critical velocity, $U = u/u_c$, and the ridge height d by the critical flow depth $h_c = Q/u_c$, to the form $D = d/h_c$. Using these scalings, Eq. (A2) becomes

$$D = \frac{U^2}{2} + \frac{1}{U} - \frac{3}{2}. \tag{A3}$$

We plotted Eq. (A3) in Fig. A1 (lower line). The curve illustrates that as the flow becomes progressively more sub- ($U<1$) or super- ($U>1$) critical, and therefore more energetic, the maximum ridge height that the whole flow can pass over increases. Note that for critical flow conditions, $U=1$, the flow as a whole cannot pass over a ridge of any elevation, since for a given steady volume flux, the critical flow corresponds to the minimum possible energy.

If the flow becomes critical at the top of the ridge, then, ahead of the ridge, the flow typically adjusts to become supercritical downstream (Fig. A1; cf. Houghton and Kasahara 1968). Flows that are critical at the ridge crest typically become supercritical downstream, because supercritical flows travel faster than gravity

waves and therefore any downstream perturbations are swept downstream and cannot affect the flow at the ridge. In contrast, if a flow that is controlled at the ridge crest were to become subcritical downstream, then any downstream perturbation could propagate back to the ridge crest and ultimately cause a transition to supercritical flow downstream.

Intermediate-size ridges – partially blocked flow

If the flow has insufficient energy to surmount a ridge crest *en masse*, then a fraction of the flow will be reflected from the ridge as a bore (Figs. A2, A3). Figure 3b illustrates a flow that is partially blocked by a ridge, which therefore produces a backward-travelling bore. The fraction of the flow that can pass over the ridge may be estimated in a fashion analogous to the blocking of wind over mountain ridges (e.g. Houghton and Kasahara 1936; Yih and Guha 1955; Baines 1984) by combining (a) the conservation of mass and momentum in the upstream bore, and (b) the condition that the flow is critical at the ridge crest (cf. Houghton and Kasahara 1968). If the depth upstream of the bore is less than approximately twice that downstream of the bore, there is very little mixing of the overlying fluid into the bore (e.g. Wood and Simpson 1984), and we may neglect such entrainment. For convenience, let us define the initial flow to be of depth h and speed u, the bore to be of depth b and speed v, and the flow downstream of the bore to be of speed w and depth $h+b$ (Fig. A2)

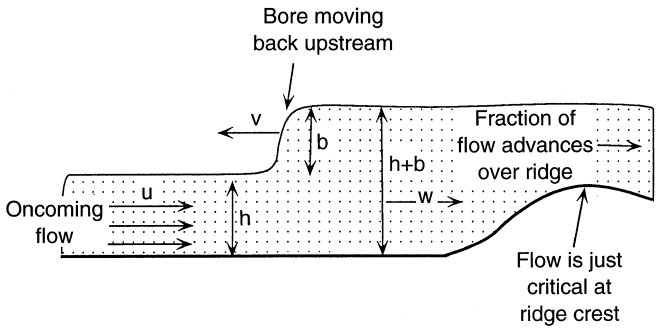

Fig. A2 Diagram defining the properties of the upstream propagating bore and the controlled flow over the ridge

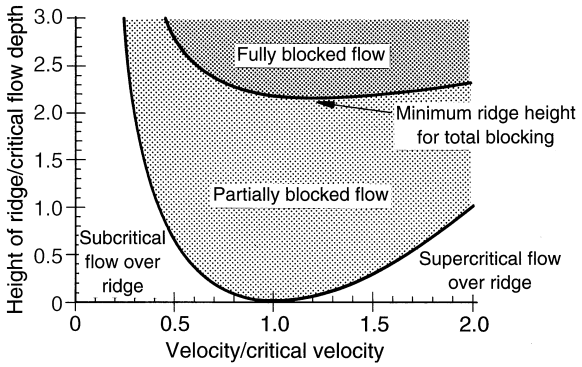

Fig. A3 Illustration of the maximum height at which all the flow can pass over a ridge (*lower line*) and of the minimum height at which all of the flow is blocked by ridge (*upper line*) as a function of the velocity of the flow. The height has been divided by the depth of the critical flow, and the velocity divided by the speed of the critical flow

Flow downstream of the bore

The flux passing over the ridge has magnitude

$$Q_r = w(h+b). \tag{A4}$$

This flow is critical at the ridge crest, and therefore at the crest it has speed

$$w = w_c = (g' Q_r)^{1/3}. \tag{A5}$$

Equating the value of the Bernoulli integral upstream of the ridge but downstream of the bore (Fig. A2) with that at the ridge crest (cf. Eq. (A2)) leads to the relationship between w, $h+b$ and the height of the ridge d:

$$g' d = \frac{w^2}{2} + \frac{g' Q_r}{w} - \frac{3}{2}(g' Q_r)^{2/3}. \tag{A6}$$

Motion of the bore

In steady state, the bore moves upstream with a constant speed v. The conservation of mass across the bore therefore has the form

$$uh = vb + w(h+b). \tag{A7}$$

The equations of motion in the frame of the steady bore are the same as in the laboratory frame. Working in the frame of the bore, the equation for the conservation of momentum, Eq. (3), may be conveniently integrated over a control volume including the bore, and leads to the relationship

$$2(u+v)^2 h + g' h^2 = 2(v+w)^2 (h+b) + g'(h+b)^2. \tag{A8}$$

We may combine these equations to relate the value of w, b and v to the flow speed and depth far upstream, u and h, as well as to the height of the ridge d. The equations may be simplified by scaling v and w with respect to u, b with respect to h, u with respect to the critical velocity, u_c, and the depths h and d with respect to h_c (Eq. (A1)). Denoting these dimensionless velocities by $U = u/u_c$, $W = w/u$ and $V = v/u$ and the dimensionless depths of the bore and ridge by $D_b = b/h$, $D = d/h_c$, the system of equations reduces to three nonlinear relations. The conservation of momentum across the bore becomes

$$2U^3(1-W)^2(1+D_b) = D_b^2(2+D_b) \tag{A9}$$

The condition that the flow is critical at the ridge crest becomes (cf. Eq. (A2))

$$W^2 U^2 2 + \frac{1+D_b}{U} = \frac{3}{2}[(1+D_b)W]^{2/3} + D \tag{A10}$$

Finally, the conservation of mass has the form

$$W = \frac{1 - VD_b}{1 + D_b}. \quad \text{(A11)}$$

Two important results follow from these equations. Firstly, we can recover the limit that all the flow passes over the ridge Eq. (A2) so that $V=0$, $W=1$, $D_b=0$, and (cf. Eq. (A3))

$$\frac{U^2}{2} + \frac{1}{U} = \frac{3}{2} + D. \quad \text{(A12)}$$

Secondly, we can deduce the limit that all of the flow is blocked by the ridge.

High ridges – complete blocking of the flow

When the ridge is just high enough to totally block the flow, no flow passes over the ridge, $W=0$, and all the flow is reflected from the ridge, $VD_b=1$. The minimum ridge height that causes total blocking may be found by equating the top surface of the bore with the height of the ridge crest, $D_b=UD-1$. This critical ridge height for total blocking is then related to the upstream flow according to

$$2U^4D = (U^2D^2 - 1)(UD - 1). \quad \text{(A13)}$$

Figure A3 shows the minimum ridge height required to totally block the flow as a function of the upstream flow speed. It is seen that the ridge height required to totally block the flow varies with U and D and has a minimum at $D=2.1$, $U=1.1$.

The totally or partially blocked flow regimes may be transient. If the flow continues for a sufficient time so that the bore can propagate back upstream to the source, then subsequently the fluid layer upstream of the ridge will continue to deepen until eventually all the flux is able to pass over the ridge, with the flow again being just eritical at the ridge crest (see Fig. 9). Only at this point does the flow issuing downstream of the ridge have the same flux as that issuing from the source. During this deepening, there will be a significant amount of sedimentation (see Sedimentation over topographic obstacles), which may lead to the development of large valley-ponded deposits.

References

Aramaki S, Ui T (1966) The Aira and Ata pyroclastic flows and related caldera depressions in southern Kyushu, Japan. Bull Volcanol 129:29–47

Baines PG (1984) A unified description of two-layer flow over topography. J Fluid Mech 146:127–167

Bonnecaze R, Hallworth M, Lister J, Huppert HE (1995) Axisymmetric particle-driven gravity currents. J Fluid Mech 294:95–131

Brantley SR, Waitt RB (1988) Interrelations among pyroclastic surge, pyroclastic flow, and lahars in the Smith Creek valley during first minutes of 18 May 1980 eruption of Mount St. Helens, USA. Bull Volcanol 50:304–326

Bursik MI, Woods AW (1996) The dynamics and thermodynamics of ash flows. Bull Volcanol 58:175–193

Dade WB, Huppert HE (1996) Emplacement of the Taupo ignimbrite by a dilute, turbulent flow. Nature 381:509–512

Druitt T (1992) Emplacement of the May 18 1980 lateral blast ENE of Mt. St. Helens. Bull Volcanol 54:554–572

Ellison TH, Turner JS (1959) Turbulent entrainment in stratified flows. J Fluid Mech 6:423–448

Fisher RV (1990) Transport and deposition of a pyroclastic surge across an area of high relief: the 18 May 1980 eruption of Mount St. Helens, Washington. Geol Soc Am Bull 102:1038–1054

Freundt A, Schminke HU (1985) Lithic-enriched segregation bodies in pyroclastic flow deposits of Laacher See Volcano (E-Eifel, Germany). J Volcanol Geotherm Res 25:193–224

Giordano G, Dobran F (1994) Computer simulations of the Tuscaloano Artemisio's second pyroclastic flow unit (Alban Hills). J Volcanol Geotherm Res 61:69–94

Hazen A (1904) On sedimentation. Trans Am Soc Civ Eng 3:45–88

Hoblitt RP, Miller CD, Vallance JW (1981) Origin and stratigraphy of the deposit produced by the May 18 directed blast. In: Lipman PW, Mullineaux DR (eds) The 1980 eruptions of Mount St. Helens, Washington. US Geol Surv Prof Pap 1250:401–419

Houghton DD, Kasahara A (1968) Nonlinear shallow fluid flow over an isolated ridge. Comm Pure Appl Math XXI:1–23

Kneller B, Edward D, McCaffrey W, Moore R (1991) Oblique reflection of turbidity currents. Geology 14:250–252

Lane- Serff G, Beal LM, Hadfield TD (1995) Gravity current flow over ridges. J Fluid Mech 292:39–53

Levine AH, Kieffer SW (1991) Hydraulics of the August 7, 1980 pyroclastic flow at Mt. St. Helens. Geology 19:1121–1124

Miller TP, Smith RL (1977) Spectacular mobility of ash flows around Anuachek and Fisher calderas. Alaska Geology 5:173–176

Schlicting H (1979) Boundary-layer theory. McGraw Hill, New York, pp 1–817

Sparks RSJ, Wilson L, Hulme G (1978) Theoretical modelling of the generation, movement and emplacement of pyroclastic flows by column collapse. J Geophys Res 83:1727–1739

Turner JS (1979) Buoyancy effects in fluids. Cambridge University Press, Cambridge

Valentine G (1987) Stratified flow in pyroclastic surges. Bull Volcanol 49:616–630

Valentine G, Wohletz K (1989) Numerical models of plinian eruption columns and pyroclastic flows. J Geophys Res 94:1867–1887

Valentine G, Wohletz K, Kieffer S (1992) Effects of topography on facies and compositional variation in caldera-related ignimbrite. Geol Soc Am Bull 104:154–165

Waitt RB (1981) Devastating pyroclastic density flow and attendant air fall of May 18: stratigraphy and sedimentology of deposits. In: Lipman PW, Mullineaux DR (eds) The 1980 eruptions of Mount St. Helens, Washington. US Geol Surv Prof Pap 1250:601–616

Walkers GPL (1983) Ignimbrite types and ignimbrite problems, J Volcanol Geotherm Res 17:65–88

Walker GPL, McBroome LA (1983) Mount St. Helens 1980 and Mount Pelee 1902. Flow or surge? Geology 11:571–574

Wilkinson DL, Wood IR (1971) A rapidly varied flow phenomenon in a two-layer flow. J Fluid Mech 47:241–256

Wilson CJN, Walker GPL (1985) The Taupo eruption, New Zealand. I. General aspects. Phil Trans R Soc Lond A314:199–218

Wood IR, Simpson JE (1984) Jumps in layered miscible fluids. J Fluid Mech 140:329–342

Woods AW, Bursik MI (1994) A laboratory study of ash flows. J Geophys Res 99:4375–4394

Yih CS, Guha CR (1955) Hydraulic jumps in a fluid system of two layers. Tellus 7:358–366